spectra. The conventional approach improves the resolution in 2D NMR spectra by increasing the digital resolution and by using strong resolution enhancement digital filtering functions at the expense of sensitivity. The new approach presented in this paper improves the resolution by increasing the dimensionality of the spectrum and simultaneously yields important additional information about the system (that is, ^{15}N and ^{13}C chemical shifts). This approach is much less sensitive to wide line widths associated with larger proteins. Indeed, it can easily be calculated that 4D spectra with virtual lack of resonance overlap and good sensitivity can be recorded for proteins as large as 40 kD. Because the resolution in the 4D spectrum shown is limited by digitization, spectra with equivalent resolution can be recorded at magnetic field strengths significantly lower than 600 MHz (14.1 T). Indeed, the inherent resolution of 4D NMR spectroscopy is so high that 4D NMR spectra should be completely analyzable even at low digitization by automated procedures. Finally, we note that the present 4D data set has been processed in only a very coarse manner by Fourier transformation of severely truncated signals. It is expected that spectra of far superior quality could be obtained in much shortened measuring times with more sophisticated data processing algorithms based on linear prediction (*19*). Indeed, such an approach should open the practical possibility for yet a further increase in dimensionality.

REFERENCES AND NOTES

1. Abbreviations: NMR, nuclear magnetic resonance; NOE, nuclear Overhauser effect; NOESY, nuclear Overhauser enhancement spectroscopy; HMQC, heteronuclear multiple quantum coherence; HOHAHA, homonuclear Hartmann-Hahn; IL-1β, interleukin-1β.
2. G. M. Clore and A. M. Gronenborn, *CRC Crit. Rev. Biochem. Mol. Biol.* **24**, 479 (1989); K. Wüthrich, *Acc. Chem. Res.* **22**, 36 (1989); G. M. Clore and A. M. Gronenborn, *Ann. Rev. Biophys. Chem.*, in press.
3. P. C. Driscoll, A. M. Gronenborn, L. Beress, G. M. Clore, *Biochemistry* **28**, 2188 (1989); P. J. Kraulis *et al.*, *ibid.*, p. 7241; G. M. Clore, E. Appella, M. Yamada, K. Matsushima, A. M. Gronenborn, *ibid.* **29**, 1689 (1990).
4. A. D. Kline, W. Braun, K. Wüthrich, *J. Mol. Biol.* **204**, 675 (1988); Y. Q. Qian *et al.*, *Cell* **59**, 573 (1989).
5. K. Wüthrich, *NMR of Proteins* (Wiley, New York, 1986); G. M. Clore and A. M. Gronenborn, *Prot. Eng.* **1**, 275 (1987).
6. C. Griesinger, O. W. Sørensen, R. R. Ernst, *J. Magn. Reson.* **73**, 574 (1987); H. Oschkinat *et al.*, *Nature* **332**, 374 (1988).
7. B. H. Oh, W. M. Westler, P. Darba, J. L. Markley, *Science* **240**, 908 (1988).
8. S. W. Fesik and E. R. P. Zuiderweg, *J. Magn. Reson.* **78**, 588 (1988); D. Marion, L. E. Kay, S. W. Sparks, D. A. Torchia, A. Bax, *J. Am. Chem. Soc.* **111**, 1515 (1989); E. R. P. Zuiderweg and S. W. Fesik, *Biochemistry* **28**, 2387 (1989).
9. D. Marion *et al.*, *Biochemistry* **28**, 6150 (1989).
10. L. E. Kay, M. Ikura, A. Bax, *J. Am. Chem. Soc.* **112**, 888 (1989); A. Bax *et al.*, *J. Magn. Reson.* **86**, 620 (1990).
11. S. W. Fesik *et al.*, *J. Am. Chem. Soc.* **112**, 886 (1989).
12. A. Bax, G. M. Clore, A. M. Gronenborn, *J. Magn. Reson.*, in press.
13. L. E. Kay, M. Ikura, R. Tschudin, A. Bax, *ibid.*, in press; M. Ikura, L. E. Kay, A. Bax, *Biochemistry* **29**, 4659 (1990).
14. P. C. Driscoll, G. M. Clore, D. Marion, P. T. Wingfield, A. M. Gronenborn, *Biochemistry* **29**, 3542 (1990); G. M. Clore, A. Bax, P. C. Driscoll, P. T. Wingfield, A. M. Gronenborn, *ibid.*, p. 4668.
15. J. J. Oppenheim, E. J. Kovacs, K. Matsushima, S. K. Durum, *Immunol. Today* **7**, 45 (1986); C. A. Dinarello, *Ann. N.Y. Acad. Sci.* **546**, 122 (1988); M. A. S. Moore, *Immunol. Res.* **8**, 165 (1989).
16. R. R. Ernst, G. Bodenhausen, A. Wokaun, *Principles of Nuclear Magnetic Resonance in One and Two Dimensions* (Clarendon, Oxford, 1987).
17. L. Mueller, *J. Am. Chem. Soc.* **101**, 4481 (1979); A. Bax, R. H. Griffey, B. L. Hawkins, *J. Magn. Reson.* **55**, 301 (1983).
18. L. E. Kay, D. Marion, A. Bax, *J. Magn. Reson.* **84**, 72 (1989).
19. H. Gesmar and J. J. Led, *ibid.* **76**, 183 (1988).
20. A. J. Shaka, J. Keeler, T. Frenkiel, R. Freeman, *ibid.* **52**, 335 (1983).
21. D. Marion, M. Ikura, R. Tschudin, A. Bax, *ibid.* **85**, 393 (1989).
22. D. Marion, M. Ikura, A. Bax, *ibid.* **84**, 425 (1989).

23. We thank P. Wingfield for preparing the sample of ^{15}N-^{13}C-labeled interleukin-1β and R. Tschudin for valuable technical support. Supported by the Intramural AIDS Antiviral Program of the Office of the Director of the National Institutes of Health (A.M.G., G.M.C., and A.B.). L.E.K. acknowledges a postdoctoral fellowship from the Medical Research Council of Canada and the Alberta Heritage Trust Foundation.

4 April 1990; accepted May 1990

Prevention of Activated Neutrophil Adhesion to Endothelium by Soluble Adhesion Protein GMP140

JENNIFER R. GAMBLE, MICHAEL P. SKINNER, MICHAEL C. BERNDT, MATHEW A. VADAS*

Neutrophils and monocytes, but not lymphocytes, adhered strongly to plastic surfaces coated with GMP140, a protein of endothelial cells and platelets. This adhesion of neutrophils was mediated by GMP140 and not by the CD18 integrin complex. By contrast, GMP140 in solution inhibited the CD18-dependent adhesion of tumor necrosis factor–α–activated neutrophils to plastic surfaces and resting endothelium, but not of resting neutrophils to tumor necrosis factor–α–activated endothelium. Thus, the binding of a soluble form of an adhesion protein selectively inhibited another set of adhesive events. Soluble GMP140 may be important in maintaining the nonadhesiveness of neutrophils in the circulation and may serve to limit inflammatory reactions.

DURING INFLAMMATION, CIRCULATING blood cells adhere to patches of endothelium and migrate into tissues. This process is regulated by cytokines such as tumor necrosis factor–α (TNF-α) and is mediated by adhesion proteins, some of which belong to the LEC-CAM (lectin–epidermal growth factor–complement binding cell adhesion molecule) family (*1*). GMP140, a glycoprotein of 140 kD, is present in the alpha granules of platelets and the Weibel Palade bodies of endothelial cells (ECs) (*2–4*). Analysis of the cDNA suggests three possible forms of GMP140: two transmembrane forms (with complement binding regions of different lengths) and a soluble form, with the transmembrane domain deleted (*2*). Upon platelet activation or treatment of ECs with thrombin or histamine, the secretory granules are rapidly exocytosed, resulting in a redistribution of transmembrane GMP140 into the plasma membrane (*5–7*). Endothelial GMP140 has structural similarity to adhesion molecules ELAM-1 (endothelial leukocyte adhesion molecule–1) and MEL-14, which belong to the LEC-CAM family (*2, 8, 9*). ELAM-1, although not present on resting endothelium, mediates adhesion of neutrophils [polymorphonuclear leukocytes (PMNs)] to endothelium activated by TNF or interleukin-1 (IL-1) (*10*). MEL-14, present on PMNs and lymphocytes, is involved in lymphocyte homing to high endothelial venules (*11*). We used platelet GMP140 that was purified to homogeneity (*12*) to investigate its role in adhesive phenomena, and our data suggest that elaboration or secretion of GMP140 serves to prevent adhesion and the development of inflammatory responses.

GMP140 was coated onto plastic microtiter wells and was adhesive for freshly isolated, nonactivated PMNs and monocytes, but not T lymphocytes (Fig. 1A). Adhesion was concentration-dependent (Fig. 1A), and the

J. R. Gamble and M. A. Vadas, Division of Human Immunology, Institute of Medical and Veterinary Science, Frome Road, Adelaide, South Australia, 5000. M. P. Skinner and M. C. Berndt, Research Centre for Thrombosis and Cardiovascular Disease, Department of Medicine, Westmead Hospital, New South Wales 2006.

*To whom correspondence should be addressed.

adhesion of PMNs was inhibited by affinity-purified rabbit Fab fragments of the antibody to GMP140 (Fig. 1B). Thus, immobilized GMP140 can promote the selective adhesion of leukocytes. The adhesion of PMNs to GMP140 was not dependent on the CD18 adhesion complex (Fig. 1B), as antibodies to the α chain of Mac-1 (CD11b) or to the common β chain (CD18) did not inhibit adhesion.

The effect of soluble GMP140 on the adhesion of PMNs to human umbilical vein ECs was investigated. Monolayers of ECs were incubated with PMNs for 30 min either in the presence or absence of TNF-α. Soluble GMP140 was also simultaneously added to some groups (Fig. 2A). GMP140 prevented TNF-α–stimulated PMN adhesion to ECs in a concentration-dependent manner (Fig. 2A). In experiments with significant basal adhesion (that is, PMNs that were not intentionally stimulated), GMP140 was also inhibitory (*13*). The effect of soluble GMP140 on PMN adhesion to TNF-α–stimulated ECs was also investigated. In contrast to the TNF-α–stimulated PMNs' adhesion to resting ECs, the adhesion of resting PMNs to TNF-α–stimulated ECs was not inhibited by GMP140 (Fig. 2B).

The effect of GMP140 on PMN adherence was a result of binding to the PMNs, because pretreatment and washing of the PMNs but not the ECs with GMP140

Table 1. PMN adhesion to ECs is inhibited by GMP140 action on the PMNs. In experiment A, PMNs (15×10^8) were first incubated with GMP140 (8 μg/ml) or medium in 300 μl for 15 min at 37°C. The tubes were then placed on ice, diluted with cold assay medium, and spun for 15 s at 12,000*g*. The cells were resuspended in assay medium and added to ECs either with or without the addition of TNF-α (10 U/ml). Parallel experiments with GMP140 added directly to the assay are also shown. Percent adhesion is expressed as the mean ± SEM of triplicate determinations and is representative of three similar experiments. No decrease in cell number or viability was observed with this protocol between groups receiving GMP140 or those with medium alone. The inhibition seen when PMNs were treated with GMP140 before the assay was consistently significant, but less than the inhibition seen when GMP140 was included in the assay. In experiment B, the ECs were treated with GMP140 or medium before the assay. EC monolayers were washed once and incubated with either GMP140 (8 μg/ml) or medium alone for 15 min at 37°C. The wells were then washed in ice-cold assay medium, and PMNs were added and assayed as in experiment A. No change in cell morphology, monolayer integrity, or uptake of Rose Bengal stain was observed with ECs treated in this way. This is a representative of three similar experiments.

Experiment	Percent adherence to EC monolayers with GMP140 added	
	Before assay	During assay
A PMN only	1.2 ± 1.0	2.4 ± 1.2
PMN + TNF-α	72.9 ± 5.4	72.5 ± 1.8
PMN + TNF-α + GMP140	51.6 ± 0.1*	20.7 ± 1.8†
B PMN only	1.7 ± 0.5	3.9 ± 2.0
PMN + TNF-α	59.8 ± 0.1	61.0 ± 1.1
PMN + TNF-α + GMP140	58.9 ± 0.8	27.6 ± 2.4‡

*$P < 0.05$ compared to group stimulated with TNF-α but not receiving GMP140. †$P < 0.001$ compared to group stimulated with TNF-α but not receiving GMP140. ‡$P < 0.02$ compared to group stimulated with TNF-α but not receiving GMP140.

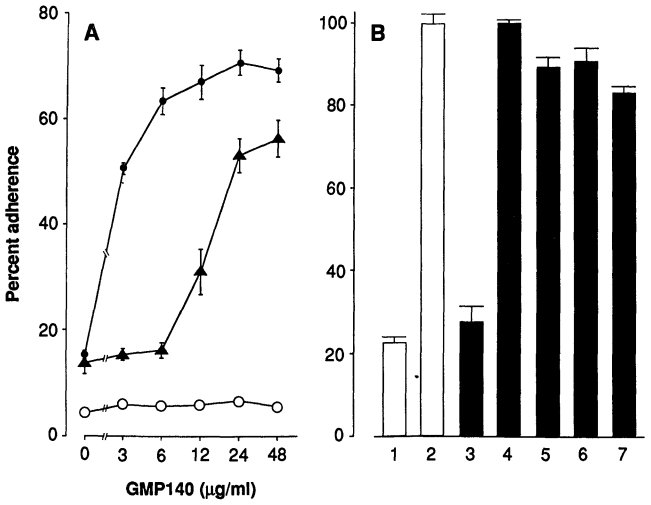

Fig. 1. (**A**) Effect of GMP140 on the adherence of PMNs, lymphocytes, and monocytes to plastic. Various concentrations of GMP140 diluted in phosphate-buffered saline, pH 7.3, were added to microtiter wells at room temperature. After 4 hours the wells were washed in assay medium (RPMI containing 2.5% fetal bovine serum). PMNs (5×10^5) (▲), T lymphocytes (○), or 2×10^5 monocytes (●) were added, incubated for 30 min, and adherence was determined. The results of individual experiments are shown and are representative of three or four experiments performed with each cell type (arithmetic mean of triplicate determinations ± SEM). The relative adhesion of PMNs and monocytes varied among the different donors. In parallel experiments, T lymphocyte adhesion to plastic could be induced by phorbol myristate acetate (10 ng/ml) (*13*). Purified GMP140 was isolated as described (*12*). The glycoprotein was stored at −70°C in 0.02 M tris buffer, 0.15 M NaCl, 0.1% Triton X-100, and 0.001 M $CaCl_2$ (buffer pH 7.4). Before use, the preparation was separated on an Extracti-Gel D column (Pierce Chemicals) to remove the Triton X-100. GMP140 was eluted in the void volume, and ~50% of the loaded protein was recovered and used within 24 hours. Monocytes were purified, and their adherence was assayed as in (*34*), PMNs as in (*35*), and T cells as in (*35, 36*). The absorbance at 570 nm (A_{570}) was determined for known numbers of Rose Bengal–stained ethanol-lysed PMNs and T cells, and a standard curve was obtained. A linear relation exists between A_{570} and number of cells attached, and from this the percent adhesion can be calculated. (**B**) Effect of antibodies on PMN adhesion to GMP140 immobilized on plastic. (Bar 1) Plastic without GMP140 coating. All other wells coated with GMP140; (bar 2) GMP140 only. Additions: (bar 3) affinity-purified rabbit anti-GMP140 Fab fragment and (bar 4) rabbit non-immune Fab fragment were used at a concentration of 20 μg/ml. (Bar 5) Control antibody 60.5 (anti-HLA) and monoclonal antibodies (bar 6) 60.3 (anti-β chain of CD18 complex), and (bar 7) 60.1 (anti-Mac-1) were used at a final concentration of 1:400 of ascites, which gives maximal inhibition in CD18-dependent adhesion assays. Results have been normalized relative to the level of adhesion to GMP140-coated plastic as 100% (bar 2).

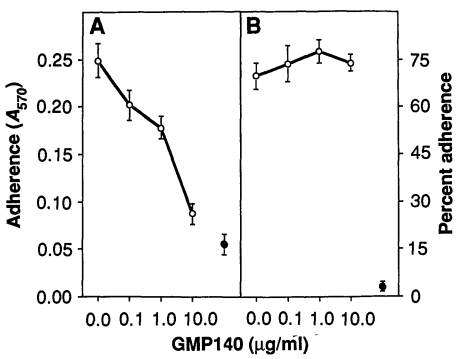

Fig. 2. The effect of GMP140 on PMN adherence to EC monolayers. Endothelial cells were harvested from human umbilical veins by collagenase treatment and grown as described (*37*) without the addition of EC growth factor and heparin. Two to 6 days after establishment of culture, ECs were harvested by trypsin-EDTA and replated into gelatin-coated microtiter wells at 2×10^4 cells per well and grown to confluency overnight. PMNs (5×10^5) were added to EC monolayers, and adhesion was measured after 30 min. (**A**) PMNs were incubated with TNF-α (10 U/ml) and graded loss of GMP140 (○). The basal level of adhesion of unstimulated PMNs to unstimulated endothelium is also shown (●). The results shown are from a single experiment which is representative of eight experiments where the average percent inhibition of TNF-α–stimulated adherence to ECs was 19, 41, and 78% for 0.1, 1.0, and 10 μg of GMP140 per milliliter, respectively. Groups receiving 1.0 and 10 μg of GMP140 per milliliter were significantly different (at $P < 0.001$) from the group not receiving GMP140 (level of significance = 0.025, Bonferroni correction). (**B**) ECs were stimulated with TNF-α (100 U/ml) for 4 hours before washing. PMNs were then added with graded doses of GMP140 (○). The basal level of adhesion of unstimulated PMN to unstimulated endothelium is also shown (●). The results shown are representative of four experiments where average inhibition was 2, 5, and 11%, for 0.1, 1.0, and 10 μg of GMP140 per milliliter, respectively (not significantly different from the group not receiving GMP140, level of significance = 0.016, Bonferroni correction).

resulted in significant inhibition of adhesion (Table 1). The inhibition of adhesion was transient (Table 1) (*13*). GMP140 did not inhibit TNF-α–activated PMN adhesion by interfering with the capacity of TNF-α to bind its receptor: treatment of the PMNs with TNF-α before addition of GMP140 still resulted in significant inhibition of adhesion to EC monolayers (Table 2, experiment A). The inhibition by GMP140 was blocked by a specific antibody and by boiling the protein (Table 2, experiments B and C), suggesting that GMP140, and not a contaminant, was mediating the effect. Inhibition by GMP140 required the presence of GMP140 from the beginning of the assay. Once the PMNs had contacted the ECs GMP140 had no effect on adhesion (Table 2, experiment D), showing that GMP140 inhibits PMN adhesion, but does not, in static adhesion assays, cause PMN detachment from ECs.

The adhesion of stimulated PMNs to endothelium is mediated through the CD18 complex [lymphocyte function–associated antigen-1 (LFA-1), Mac-1, and p150,95] of adhesion glycoproteins on the PMNs, particularly by CD11b/CD18 (Mac-1) and CD11a/CD18 (LFA-1) (*14–18*). The ligand for LFA-1 is intercellular adhesion molecule–1 (ICAM-1) (*19, 20*); the ligand for Mac-1 on the endothelium is unknown, but may also partially involve ICAM-1 (*21*). After activation of PMNs with agents such as TNF-α, C5a, and lipopolysaccharide, the expression or conformational state (*22–24*) of these molecules is altered. PMNs become more adhesive (*14, 22–25*), which is a transient state (*25*) and by itself does not lead to transmigration (*26*). More than 95% of this adhesion to EC is blocked by antibodies to the CD18 complex (*27*) and, as shown here, by the glycoprotein GMP140. Adherence of TNF-α–activated PMNs to plastic is also totally Mac-1–dependent (*27*), and soluble GMP140 also inhibits this adhesion (Table 3). Since adhesion to immobilized GMP140 is not CD18-dependent, this work suggests that GMP140 inhibits at least the Mac-1–dependent process of PMNs.

Table 3. The effect of soluble GMP140 on PMN adhesion to plastic surfaces. Soluble GMP140 was added to PMNs in plastic microtiter wells 2 min before activation with TNF-α (10 U/ml), and adhesion was determined 30 min later. The percent adhesion ± SEM of triplicate determinations of one experiment representative of two such experiments is shown.

GMP140	Activation	Percent adherence
Nil	Nil	5.4 ± 0.6
Nil	TNF-α	26.2 ± 1.0
2.5 μg/ml	TNF-α	18.7 ± 0.7*
5.0 μg/ml	TNF-α	13.8 ± 0.4*

*Significantly different from group that was TNF-activated, but not receiving soluble GMP140; $P < 0.025$, level of significance = 0.025, Bonferroni correction.

Adhesion to endothelium that is activated with agents such as TNF-α and IL-1 (*14, 28*) is qualitatively different from the adhesion of activated PMNs to resting endothelium. Adhesion to activated endothelium is slower to develop, is only partially inhibited by antibodies to CD18, is mediated through the expression of a new protein ELAM-1, and possibly other ligands (*29*), on ECs, results in transmigration (*30*), and is not inhibited by GMP140. Our findings show that soluble GMP140 selectively inhibits the adhesion process of activated neutrophils to endothelium and demonstrate that the mechanism of the two types of adhesion is different.

GMP140 is expressed on endothelial cells after stimulation with thrombin and histamine (*7*) and has been implicated in the rapid adhesion of PMNs to endothelium stimulated by these agents (*31, 32*). In addition, cDNA clones have been identified that lack the transmembrane domain (*2*), suggesting that GMP140 exists in soluble form. The release of soluble GMP140 under appropriate conditions may limit the adhesion of activated PMNs to endothelium. The shedding of MEL-14 from activated PMNs has led to the hypothesis that it also may inhibit adhesion (*33*). Antiadhesive mechanisms could be important in situations in which neutrophils are activated, such as in blood infections, when either the coagulant or complement pathway is activated, or when cytokines are administered in vivo. Therapeutic administration of GMP140 may therefore be useful to limit vascular pathology.

Table 2. Characterization of GMP140 inhibition of PMN adherence to ECs. Experiment A: PMNs were incubated for 10 min at 37°C with TNF-α (10 U/ml) or medium and then added to the EC monolayers with or without GMP140 (3 μg/ml). Experiment B: GMP140 was boiled for 15 min and then added at a concentration of 10 μg/ml to the assay. Experiment C: GMP140 (3 μg/ml) was preincubated with rabbit antibody (Fab fragment, 50 μg/ml) for 30 min at room temperature and then added to the adherence assay. Experiment D: GMP140 (10 μg/ml) was either added at the same time as PMN and TNF to the EC monolayers or added 15 min later. The mean percentage adherences ± SEM of single experiments are given that are representative of at least two similar experiments performed for each.

	TNF-α addition		GMP140		Other addition	Percent adherence
	PMN pretreatment	Directly to assay	Presence	How added		
A						7.0 ± 1.2
	10 min					32.7 ± 2.9
	10 min		+			17.3 ± 1.2*
B						7.8 ± 2.6
		+				82.2 ± 3.7
		+	+			43.7 ± 3.7*
		+	+	Boiled		84.1 ± 5.2†
C						12.0 ± 2.6
		+				80.3 ± 4.7
		+	+			64.1 ± 2.6
		+	+		Anti-GMP140 Fab	84.1 ± 4.4
		+	+		Nonimmune Fab	63.5 ± 0.3‡
D						2.9 ± 1.5
		+				47.1 ± 2.9
		+	+			25.6 ± 2.1*
		+	+	15 min after start of assay		57.6 ± 6.5

*$P < 0.05$ compared to group not receiving GMP140. †$P < 0.05$ compared to group receiving unboiled GMP140. ‡$P < 0.05$ compared to group receiving anti-GMP140 Fab.

REFERENCES AND NOTES

1. M. Stoolman, *Cell* **56**, 907 (1989).
2. G. I. Johnston, R. G. Cook, R. P. McEver, *ibid.*, p. 1033.
3. G. I. Johnston, A. Kurosky, R. P. McEver, *J. Biol. Chem.* **264**, 1816 (1989).
4. R. Bonfanti, B. C. Furie, B. Furie, D. D. Wagner, *Blood* **73**, 1109 (1989).
5. P. E. Stenberg, R. P. McEver, M. A. Shuman, Y. V. Jacques, D. F. Bainton, *J. Cell. Biol.* **101**, 880 (1985).
6. R. P. McEver and M. N. Martin, *J. Biol. Chem.* **259**, 9799 (1984).
7. R. Hattori, K. K. Hamilton, R. D. Fugate, R. P. McEver, P. J. Sims, *ibid.* **264**, 7768 (1989).
8. M. P. Bevilacqua, S. Stengelin, M. A. Gimbrone, Jr., B. Seed, *Science* **243**, 1160 (1989).
9. M. H. Siegelman, M. van de Rijn, I. L. Weissman, *ibid.*, p. 1165.
10. M. P. Bevilacqua, J. S. Pober, D. L. Mendrick, R. S. Cotran, M. A. Gimbrone, Jr., *Proc. Natl. Acad. Sci. U.S.A.* **84**, 9238 (1987).
11. W. M. Gallatin, I. L. Weissman, E. C. Butcher, *Nature* **304**, 30 (1983).
12. M. P. Skinner *et al.*, *Biochem. Biophys. Res. Commun.* **164**, 1373 (1989).
13. J. R. Gamble and M. A. Vadas, unpublished observations.
14. J. R. Gamble, J. M. Harlan, S. J. Klebanoff, M. A. Vadas, *Proc. Natl. Acad. Sci. U.S.A.* **82**, 8667 (1985).
15. G. A. Zimmerman and T. M. McIntyre, *J. Clin.*

Invest. **81**, 531 (1988).
16. B. Schleiffenbaum, R. Moser, M. Patarroyo, J. Fehr, *J. Immunol.* **142**, 3537 (1989).
17. M. G. Tonnesen *et al.*, *J. Clin. Invest.* **83**, 637 (1989).
18. D. C. Anderson, L. J. Miller, F. C. Schmalstieg, R. Rothlein, T. A. Springer, *J. Immunol.* **137**, 15 (1986).
19. S. D. Marlin and T. A. Springer, *Cell* **51**, 813 (1987).
20. M. W. Makgoba *et al.*, *Nature* **331**, 86 (1988).
21. C. W. Smith, S. D. Marlin, R. Rothlein, C. Toman, D. C. Anderson, *J. Clin. Invest.* **83**, 2008 (1989).
22. J. P. Buyon *et al.*, *J. Immunol.* **140**, 3156 (1988).
23. M. R. Philips, J. P. Buyon, R. Winchester, G. Weissman, S. B. Abramson, *J. Clin. Invest.* **82**, 495 (1988).
24. N. B. Vedder and J. M. Harlan, *ibid.* **81**, 676 (1988).
25. S. K. Lo, P. A. Detmers, S. M. Levin, S. D. Wright, *J. Exp. Med.* **169**, 1779 (1989).
26. W. Smith, J. R. Gamble, M. A. Vadas, in preparation.
27. S. K. Lo, G. A. Van Seventer, S. M. Levin, S. D. Wright, *J. Immunol.* **143**, 3325 (1989).
28. M. P. Bevilacqua *et al.*, *J. Clin. Invest.* **76**, 2003 (1985).
29. F. W. Luscinskas, A. F. Brock, M. A. Arnaout, M. A. Gimbrone, Jr., *J. Immunol.* **142**, 2257 (1989).
30. R. Moser, B. Schleiffenbaum, P. Groscurth, J. Fehr, *J. Clin. Invest.* **83**, 444 (1989).
31. G. A. Zimmerman, T. M. McIntyre, S. M. Prescott, *ibid.* **76**, 2235 (1985).
32. J-G. Geng *et al.*, *Nature* **343**, 757 (1990).
33. T. K. Kishimoto, M. A. Jutila, E. L. Berg, E. C. Butcher, *Science* **245**, 1238 (1989).
34. J. R. Gamble, M. J. Elliott, E. Jaipargas, A. F. Lopez, M. A. Vadas, *Proc. Natl. Acad. Sci. U.S.A.* **86**, 7169 (1989).
35. J. R. Gamble and M. A. Vadas, *J. Immunol. Methods* **109**, 175 (1988).
36. Y. Saegusa, D. Cavender, M. Ziff, *J. Immunol.* **141**, 4140 (1988).
37. R. T. Wall, L. A. Harker, L. J. Quadracci, G. E. Striker, *J. Cell. Physiol.* **96**, 203 (1978).
38. We thank A. Lopez for helpful discussions; F. Bilogrevic and T. Browning for technical assistance; the staff of the delivery ward at The Queen Victoria Hospital, Adelaide, for collection of the umbilical cords; the staff at the Red Cross Blood Bank, Adelaide, for preparation of blood packs; Genentech, South San Francisco, for TNF-α; P. Beatty, Fred Hutchinson Cancer Center, Seattle, for the gift of the monoclonal antibodies 60.1, 60.3, and 60.5; and M. Walker and B. Meakins for manuscript preparation. Supported by grants from the National Health and Medical Research Council (NH & MRC) of Australia and the National Heart Foundation. M.P.S. is the recipient of an NH & MRC postgraduate fellowship and M.C.B. of a Wellcome Senior Research Fellowship.

5 December 1989; accepted 8 May 1990

Functional Organization of Primate Visual Cortex Revealed by High Resolution Optical Imaging

DANIEL Y. TS'O, RON D. FROSTIG, EDMUND E. LIEKE, AMIRAM GRINVALD

A high spatial resolution optical imaging system was developed to visualize cerebral cortical activity in vivo. This method is based on activity-dependent intrinsic signals and does not use voltage-sensitive dyes. Images of the living monkey striate (V1) and extrastriate (V2) visual cortex, taken during visual stimulation, were analyzed to yield maps of the distribution of cells with various functional properties. The cytochrome oxidase–rich blobs of V1 and the stripes of V2 were imaged in the living brain. In V2, no ocular dominance organization was seen, while regions of poor orientation tuning colocalized to every other cytochrome oxidase stripe. The orientation tuning of other regions of V2 appeared organized as modules that are larger and more uniform than those in V1.

IN THE MAMMALIAN NEOCORTEX, CELLS with similar functional properties are often grouped together into columns that run vertically from the pial surface to the white matter (*1, 2*). A striking demonstration of functional segregation can be seen in striate cortex (V1) when it is histochemically stained for cytochrome oxidase (*3*). A pattern of densely stained patches or blobs is revealed (*4*) among regions of lighter staining (interblobs). The blobs contain cells that are unoriented, monocular, and often color-selective, whereas cells in the interblobs are selective for orientation but usually not for color (*5*). A different pattern of cytochrome oxidase staining is observed in the second visual area (V2) of the primate: a series of bands or stripes. The stripes of denser staining are of two types, thick and thin, alternate in a regular fashion, and are separated by intervening lighter, or pale stripes (*6, 7*). Electrophysiological studies (*8, 9*) have shown that the thin stripes contain unoriented color cells, whereas the thick stripes contain oriented, disparity-sensitive cells.

These previous studies relied on postmortem histology to identify these cortical subdivisions and thus could not directly investigate identified cortical regions with a microelectrode. Cortical activity can now be mapped with optical imaging (*10–13*) to obtain successive maps of responses to many different stimuli from the same cortical region in vivo, follow variations in responses over time, and quickly map a relatively large cortical region.

Most in vivo optical imaging studies have used optical signals provided by voltage-sensitive dyes (*11*). However, it is desirable to avoid the use of extrinsic probes when their ability to provide higher temporal resolution is not required since the dyes may introduce several complications, including pharmacological side effects, phototoxicity, and uncertainties in staining. Here we have used a system with high spatial resolution for the optical imaging of intrinsic, activity-related optical signals (*14, 15*) in mammalian cortex. We have directly imaged, in vivo, the organization of several functional properties of cells, as well as the blobs of V1 and the stripes of V2 (*16*).

We began each experiment by acquiring an image of the cortical surface with a charge-coupled device (CCD) camera (*17–20*). This initial image served as a guide for the positioning of electrodes and a reference for cortical movement and drift over time (Fig. 1A).

To demonstrate our ability to visualize the functional architecture of visual cortex without the use of voltage-sensitive dyes, we imaged the ocular dominance (Fig. 1B) and orientation (Fig. 1C) columns of V1 (*2, 21*). In addition to single-unit recordings that confirmed our ocular dominance and orientation maps (*22*), we also saw a close correspondence between our maps and maps obtained from postmortem techniques, such as 2-deoxyglucose (2-DG) autoradiography, cytochrome oxidase histology, and anterograde tracing. Our maps of ocular dominance and orientation tuning in V1, based on intrinsic signals, are similar to the maps of Blasdel and Salama (*12*), who used voltage-sensitive dyes. We analyzed our orientation maps for "fractures," regions with rapidly changing orientation tuning. However, we did not find a consistent relationship between these fractures and the ocular dominance columns (*12*). For each orientation, we also attempted to image preferences for the direction of motion, but did not observe any differential response. These results imply that directionality is not organized in a columnar fashion.

We found that our ocular dominance maps also contained the information necessary to visualize the cytochrome oxidase blobs of

D. Y. Ts'o, R. D. Frostig, E. E. Lieke, The Laboratory of Neurobiology, The Rockefeller University, New York, NY 10021.
A. Grinvald, IBM, Research Division, Yorktown Heights, NY 10598; The Laboratory of Neurobiology, The Rockefeller University, New York, NY 10021; and the Weizmann Institute of Science, Israel.